Proceedings of ICES06
2006 Spring Technical Conferenceof the ASME Internal Combustion Engine Division
Aachen, Germany, May 8-10, 2006

DRAFT - ICES2006-1310

NO_X EMISSIONS REDUCTION OF A NATURAL GAS *SI* ENGINE UNDER LEAN CONDITIONS: COMPARISON OF THE *EGR* AND *RGR* CONCEPTS.

Le Corre Olivier
Ecole des Mines de Nantes
4 rue A. Kastler
BP 20 722 - 44 307 Nantes cedex 3 - France
Tel : +33 2 51 85 82 57;Fax : +33 2 51 85 82 99
Email : lecorre@emn.fr

Pirotais Frédéric
now at Laboratoire des Ecoulements Géophysiques et Industriels
BP 53 38041 Grenoble Cedex 9
Tel : +33 4 56 52 02 59;Fax : +33 4 56 52 02 53
Email : Frederic.Pirotais@hmg.inpg.fr

ABSTRACT

In natural gas *SI* engines under lean conditions, *NOx* emissions reduction can be realized by injecting an additional mass flow rate to inlet gases. It can be easily done in situ using two techniques: *EG*R (Exhaust Gas Recirculation) or *RGR* (Reformed Gas Recirculation) which is an improvement of the usual *EGR* configuration. Exhaust gases are catalyzed before being reintroduced at the engine inlet. Reformed gases contain carbon monoxide and hydrogen in addition to carbon dioxide, steam and nitrogen dioxide that compose usual recirculated gases. In order to compare *EGR* and *RGR* concepts, the study is divided in three stages. Firstly, a "two-zone" thermodynamic model has been developed and validated on a large open chamber *SI* engine (18L *CHP* plant engine, fuelled by natural gas and equipped with data acquisition). Both in-cylinder pressure and nitrous oxide emissions have been compared between numerical results and experimental data. A good agreement is obtained, the error is less than 0.5%. Secondly, a widespread model of steam reforming on a $Ni/MgOAl_2O_3$ catalyst has been used to compute in particular *CO* and H_2 concentrations. Numerical results lead to a good concordance with experimental data from literature. Finally, *SI* engine and reformer models have been linked. *RGR* and *EGR* configurations have been numerically compared considering the same recirculation mass flow rate. According to the results, *RGR* is the best way to decrease significantly nitrous oxide emissions, keeping good engine performances.

INTRODUCTION

Compared to others prime movers, Combined Heat and Power (*CHP*) plants based on *SI* engines and fuelled by natural gas have a good thermal efficiency and lead to a smaller impact on global warming. Moreover, the high *H/C* ratio limits the CO_2 emission level.

Nevertheless, Sogaard et al [1] bring to the fore one serious drawback of those *CHP* plants: the high emission level of unburned hydrocarbon (*UHC*), mainly methane, present in exhaust gases. Indeed methane has 21 times the *GWP* of carbon dioxide. Authors have also noticed that an addition of hydrogen in natural gas reduces the *UHC* emissions. Tsolakis and Megaritis [2] summarise the main advantages of a hydrocarbon and hydrogen blend as a fuel for *IC* engines : it increases thermal efficiency and reduces *UHC, CO,* CO_2 emissions. On the other hand, the higher hydrogen flame speed increases in-cylinder peak pressure and temperature. It raises NO_x emissions except under lean conditions.

Hydrogen is often proposed as the fuel for future since its combustion leads to a limited impact on environment compared to hydrocarbon fuels. Unfortunately, hydrogen production and storage are difficult for both stationary and mobile applications, cf. Hoekstra et al. [3]. Storage can be avoided by an in-situ production, using reformed fuels that are rich in hydrogen, like natural gas. From a chemical point of view, natural gas reforming process aims to crack hydrocarbon molecules like methane to obtain hydrogen and carbon monoxide.

Natural gas reforming is an endothermic operation that requires steam and a catalyst. Consequently, using exhaust gases to bring steam and recover thermal energy, seems to be an efficient solution, especially for *CHP* plants. The reforming device (see figure 1) is able to mix a fraction of exhaust gases and natural gas to provide heat and steam in presence of catalyst materials. Chemical reaction products are reintroduced (particularly hydrogen) towards engine inlet. Technologically,

this technique can be applied to *IC* engines incorporating the reforming reactor into the conventional *EGR* system

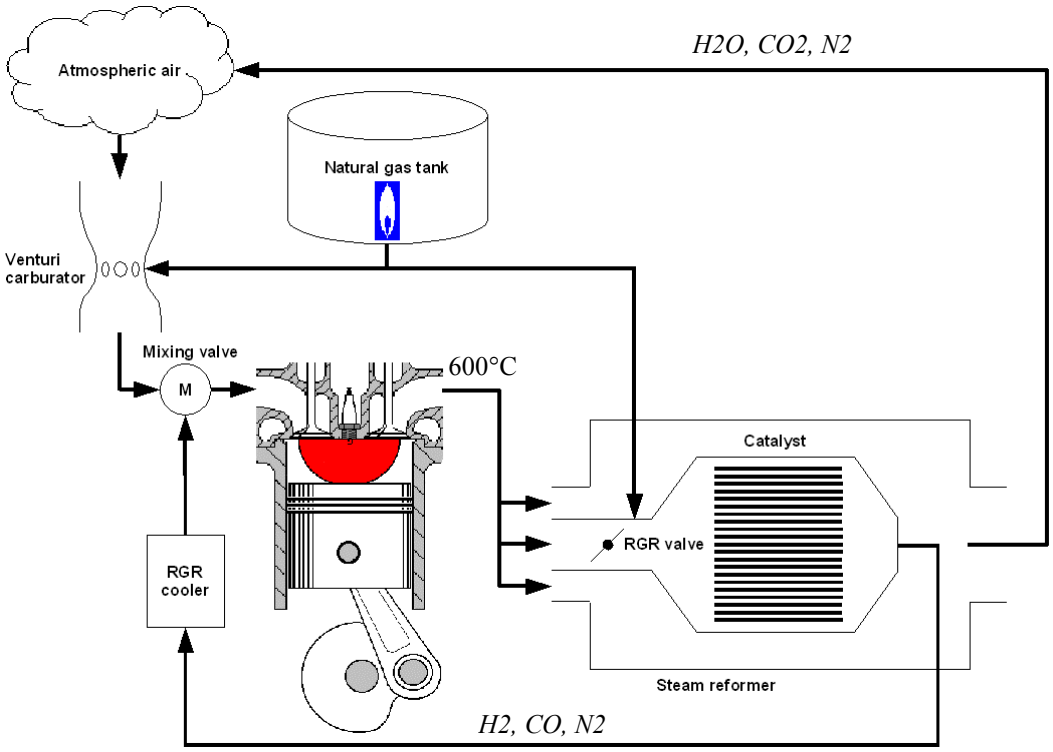

Figure 1. S.I. engine equipped with reformed gas recirculation inspirited from Zheng et al. [4]

According to Tsolakis and Megaritis [5] or Jamal et al. [6], the first engines applications of such reformers were available on compression ignited engines running under lean combustion. Similarly, *CHP* engines exhaust gases contain also a significant amount of oxygen and steam.

The aim of this paper is to predict numerically engine performances and emissions using a steam reformer to crack methane on a $Ni/MgOAl_2O_3$ catalyst. To achieve this goal, a *SI* engine thermodynamic model is developed. As it distinguishes burned and fresh gases in combustion chamber, it is often called a "two-zones" model. It has been validated on an experimental test bench. As the fuel is a hydrogen and natural gas mixture, a specific laminar speed mode is required to characterise in-cylinder rate of heat release. In a second part, a chemical reactive flow is proposed to describe the operations of the steam reformer. In the third part, both engine and reformer models are coupled. The completed model has been used to achieve numerical investigations to predict *NOx* emissions.

NOMENCLATURE

A	Exponential pre-factor	
Aff	Front flame area	
AFR	Air Fuel Ratio	
B	Bore	[m]
BTDC	Before Top Dead Center	
CA	Crank angle	
CHP	Combined Heat and Power	
C_v	volumic capacity	[J/K kg]
DEN	Denominator	
E	Activation energy	
EGR	Exhaust gas recirculation	
FAR	Fuel Air Ratio	
h	specific enthalpy	[J/kg]

1. S.I. ENGINE MODEL

1.1 *SI* ENGINE THERMODYNAMIC MODELS: STATE OF THE ART

For more than 40 years, combustion chamber thermodynamic descriptions are developed to analyse or to predict internal combustion engines performances. In this paper, a "two-zones" model has been developed. Its mathematical foundations are presented in the reference books written by Fergusson [7], Heywood [8] and Ramos [9]. Five assumptions are mainly retained:

1. Combustion chamber is divided in two zones: the first for fresh gases and the second for burned gases. Both are separated by a flame front.
2. In-cylinder temperature for each zone is assumed to be uniform. This hypothesis is realistic for fresh gases but debatable for burned gases considering the temperature gradient that exists inside the burned gases core.

h_W	hohenberg coefficient	[W/K m^2]
IC	Internal combustion	
L	Connecting rod length	[m]
m	In-cylinder mass	[kg]
p	Pressure	[Pa]
Q_p	In-cylinder heat losses	[J]
R	Ideal gas constant	[J/K Kg]
r	rate of kinetic reaction	
RGR	Reformed gas recirculation	
ROHR	Rate of Heat Release	
S	Strokes	[m]
s	Speed	[m/s]
SA	Spark advance	
SI	Spark Ignition	
T	Temperature	[K]
$\overline{U}$	Piston linear average speed	[m/s]
UHC	Unburnt hydrocarbon	
RPM	Round per minute	
u	specific internal energy	[J/kg]
V	In-cylinder volume	[m3]
WOT	Wilde Opening Throttle	
x	Conversion variable	
x_b	burnt fraction	
λ	stiochiometric ratio	
ω	Rotation speed	[RPM]
θ	Crank angle	[CA]
ρ	specific volume	[kg/m^3]
γ	capacity ratio	
Y	Combustion products	
ΔH^o	Enthalpy change	

Subscript

b	burnt
coll	collector
f	fresh
L	Laminar
T	Turbulent
u	unburnt

3. Pressure is assumed to be homogeneous in the whole combustion chamber.
4. Heat transfer between the two zones is usually neglected.
5. Leakage and blow-by can also be neglected, see Gatowski et al. [10].

The first thermodynamic law gives one energy equation for each zone. Ideal gas law supplies another one. In-cylinder global volume is computed knowing engine mechanical design. Heat transfer from each zone towards cylinder walls is evaluated by Hohenberg correlation [11]. Combustion progress is usually modelled using the burned fraction associated to the concept of heat release rate. There are two ways to evaluate the burned fraction. Firstly, behaviour models have been developed to predict burned fraction. The well-known Wiebe's function [12-19], cosine [12,20] or polynomial approaches [12,21] are mathematical functions which fit experimental data in a satisfying way. Nevertheless such models do not take into account physical and chemical phenomenon that occur during the combustion process. Consequently, specific characteristics of the hydrocarbon and hydrogen mixture are taken into account with correlations. Secondly, phenomenological models are based on physical considerations of the combustion process. In S.I. engines, burned gases zone is usually considered as a half-sphere centred on spark plug enclosed by a flame surface A_{FF}. The flame front propagation through fresh gases, of specific mass ρ_f, is governed by turbulent speed s_T. Modelling the front flame with a half-sphere is a simple hypothesis. Indeed, because of in-cylinder turbulent motions, the front flame is crumpled. Consequently, the front flame surface is higher than the hemispherical one. To be more realistic, in the smooth hemispherical front flame, turbulent motion effects are taken into account in the turbulent flame speed. This model gives good general results and particularly at high engine loads and small air-excess. For very lean conditions and low loads (i.e. very close to ignition limit), this model does not reproduce correctly experimental results. Hence, Chmela and al. [22] have proposed a new description of combustion in gas engines with large chamber. It is better adapted to *CHP* plants under lean conditions. In our approach, laminar speed is a combination of the expression proposed by Rousseau [12] for hydrocarbon and the expression proposed by Shahad Al-Janabi and Sadi Al-Baghadi [23] for hydrogen. The set of equations is given in appendix A.

1.2 TEST BENCH

In order to validate the previous combustion model, a stationary SI gas engine connected to a 210 kW electric generator has been used (see figure 2) with a test bench. Technical specifications of the engine are gathered in Table 1.

The acquisition system of in-cylinder pressure is composed of:

- A piezo electric cylinder pressure sensor – AVL QH32D, gain 25.28pC/bar, range 0-200 bar
- A charge amplifier - AVL 3066A0
- A shaft position encoder – AVL 364C
- A piezo resistive pressure sensor inside the inlet manifold with its amplifier – range 0-2.5 bar

Experimental curves of cylinder pressure versus crank angle (resolution of 0.1 CA) are averaged over 100 cycles.

1.3 VALIDATION OF THE TWO ZONES MODEL

The engine operation point of the test is characterised by the following parameters:

- full load (100% WOT: Wide Opening Throttle),
- FAR: 0.67,
- spark advance: 16°BTDC,
- engine revolution speed: 1500rpm.

Natural gas composition is given in Table 2.

Comparison is performed on the in-cylinder pressure since this is the only available in-cylinder data, see Figure 3.

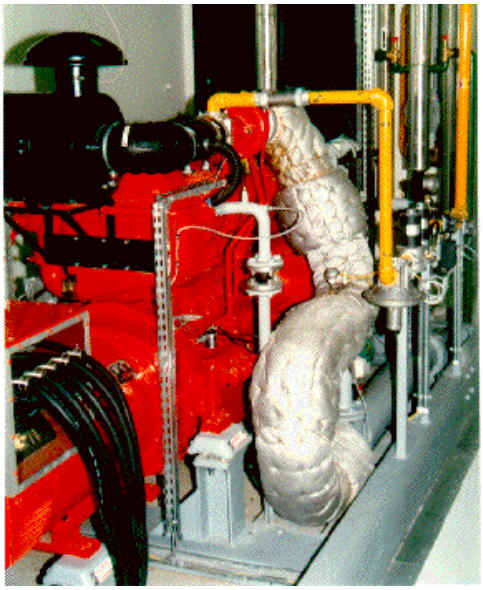

Figure 2. CHP engine fuelled by natural gas

In-cylinder fresh, burned and adiabatic flame temperatures are plotted on Figure 4. Cause of the dissociation-recombination reactions, the amount energy can be endothermic and the consequence is the flame temperature is under the burnt gas temperature, this is also reported by Leide [24]. In-cylinder mass is represented on Figure 5.

To extend the validation, different running conditions were investigated: $0.59 \le FAR \le 0.74$, $8 \le SA \le 18° BTDC$, $50\% \le Load \le 100\%\ WOT$

In the context of this paper, two criteria are analysed: the first one is the in-cylinder peak pressure and the second one is NO_x emissions. A very good agreement is obtained for the in-cylinder peak pressure for all the engine conditions, see Figure 6. A good match is obtained for the nitrogen oxide too, see Figure 7.

The thermodynamic two-zones model is validated with a good match on the experimental device (*SI* engine with large open chamber, natural gas fuelled, under lean conditions).

2. STEAM-REFORMER

Steam reforming has already been studied for furnace applications. The process carries out is conversion of natural gas (mainly considered as methane) and steam mixture to carbon monoxide and hydrogen. Details about kinetic reactions can be found in the original paper by Xu and Froment [25].

Designation	Testing Bench
Displacement Volume	*17 964 cm³*
Number of cylinders	*6*
Bore *B*	*152 mm*
Con. Rod length *L*	*300 mm*
Stroke *S*	*165 mm*
Intake opens	*25°BTC*
Intake closes	*45°ABC*
Exhaust opens	*60°BBC*
Exhaust closes	*15°ATC*
Spark timing	*12°BTC*
Engine Speed	*1500 RPM*

Table 1: Engine data

CH_4	C_2H_6	C_3H_8	C_4H_{10}	C_5H_{12}	N_2	CO_2
87.1	8.8	2.5	0.8	0	0.8	0

Table 2: Natural gas composition (in volume)

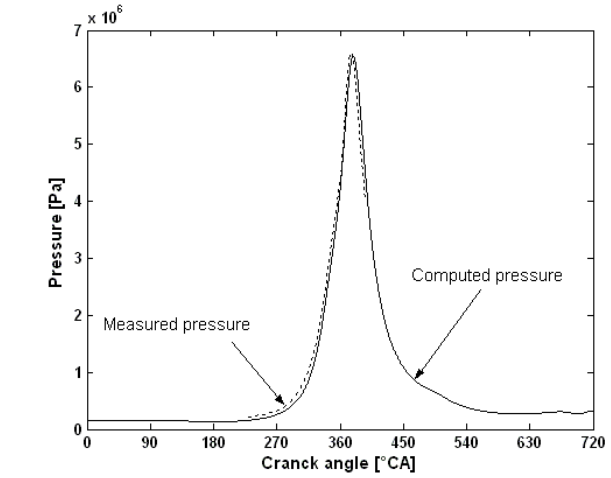

Figure 3. In-cylinder pressure comparison between measurement and simulation

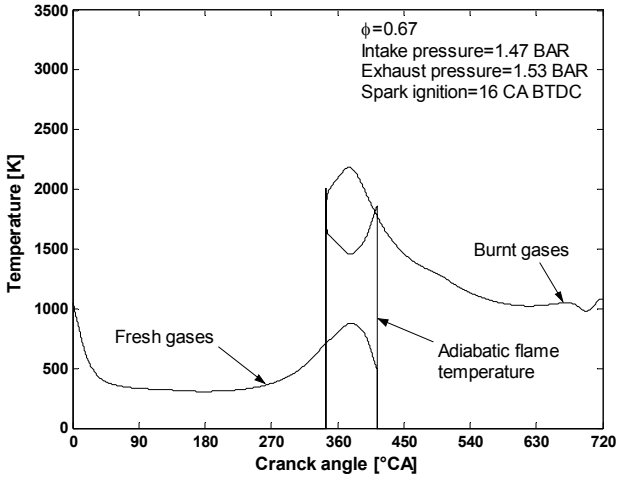

Figure 4. Estimated in-cylinder temperatures

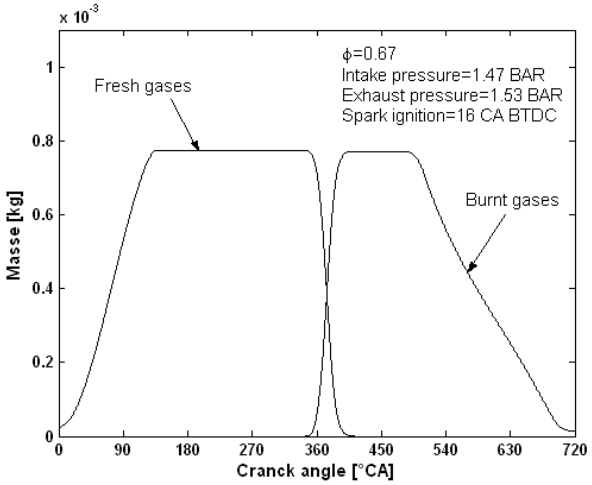

Figure 5. Estimated in-cylinder masses

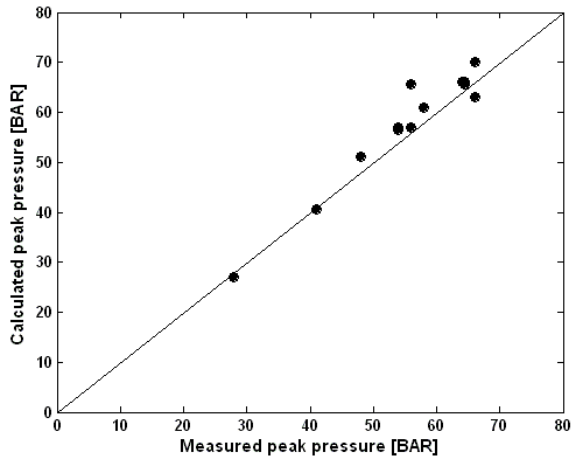

Figure 6. Numeric versus Measurement for Peak of Pressure [BAR]

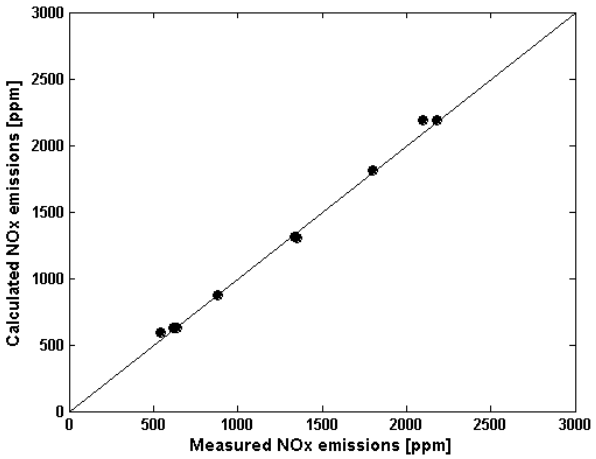

Figure 7. Numeric versus Measurement for NOx [ppm]

2.1 STATE OF ART

Nielsen et al. [26] resumed the seven common assumptions of steam reformer models:

1. A one-dimensional heterogeneous approach is used, see Froment and Bischoff [27].
2. The reactor type is assumed to be a fixed bed plug flow reactor.
3. The reformer geometry is assumed to be a pipe shaped as a straight hollow cylinder.
4. The model does not consider axial mixing.
5. All reactants are considered in the gas phase and obey the ideal gas equation of state.
6. Rather than attempt to use the actual pellet geometry, we will approximate it by a slab geometry.
7. One will only consider internal mass transport limitations, and not any heat transfer limitations, so there will be no energy balance inside the particle. This is an assumption that can often be justified, since heat transfer within the particle occurs primarily by conduction through the solid parts, while mass transfer occurs only in the pores.

2.2 MODEL AT EQUILIBRIUM

The intrinsic reaction kinetics on the surface can be represented by three reactions with Langmuir-Hinshelwood style rate expressions, see Xu and Froment [25]:

Reforming kinetic

Co-production from CH_4

$$CH_4 + H_20 = CO + 3H_2 \qquad r_1 = \frac{\frac{k_1}{p_{H_2}^{2.5}}\left(p_{CH_4}\ p_{CO_2} - \frac{p_{H_2}^3\ p_{CO}}{K_1}\right)}{DEN^2}$$

Water-gas shift

$$CO + H_2O = CO_2 + H_2 \qquad r_2 = \frac{\frac{k_2}{p_{H_2}}\left(p_{CO}\ p_{H_20} - \frac{p_{H_2}\ p_{CO_2}}{K_2}\right)}{DEN^2}$$

Production of CO_2 from CH_4

$$CH_4 + 2H_2O = CO_2 + 4H_2 \qquad r_3 = \frac{\frac{k_3}{p_{H_2}^{3.5}}\left(p_{CH_4}\ p_{H_2O}^2 - \frac{p_{H_2}^2\ p_{CO}}{K_3}\right)}{DEN^2}$$

With:

$$DEN = 1 + K_{CO}\ p_{CO} + K_{H_2}\ p_{H_2} + K_{CH_4}\ p_{CH_4} + \left(\frac{K_{H_2O}\ p_{H_2O}}{p_{H_2}}\right)$$

The water gas shift is exothermic, the two other are endothermic. The rate of disappearance of methane is calculated from: $R_{CH_4} = r_1 + r_3$. Both the absorption constants and the rate constants are found using a Arrhenius type equation:

$$K_i = A(K_i)\exp\left(\frac{-\Delta H_i^0}{R\,T}\right) \text{ and } k_j = A_j \exp\left(\frac{-E_{a,j}}{R\,T}\right)$$

de Groote and Froment [28] supply the different constants for steam reforming of methane on a $NI/MgOAl_2O_3$ catalyst.

Figure 8 proposes the equilibrium mole fraction of reformed species versus the equilibrium temperature for a reformer inlet pressure taken as 1.8 BAR. Let us underline that a turbo-charged CHP based on engine reaches those manifold pressure and a temperature around 800K (assuming a correct heat protection). The mole fraction of nitrogen decreases since the total mole fraction increases, but the value is constant.

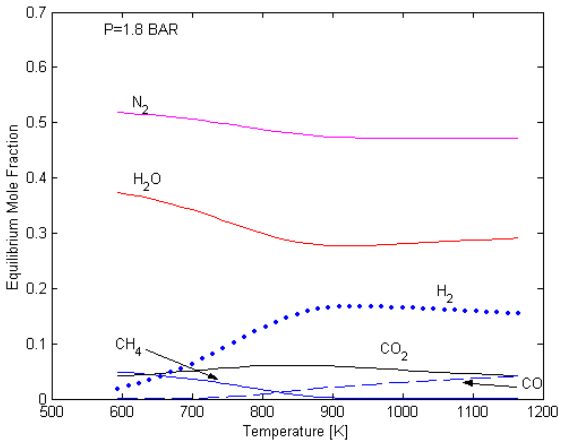

Figure 8. Equilibrium mole fraction of reformed species versus temperature

2.3 STEAM REFORMING MODEL

In steam reformer, the flow-rate is composed by natural gas and exhaust gas (from *IC* engine). Since only two of the three kinetic reactions are linearly independent, the two first one are considered. The conversion variable x is defined for a specie s as:

$$x_s = \frac{F_s^o - F_s}{F_{CH_4}^o}$$

Taking methane and carbon dioxide as independent variables, the following relations are obtained from the two first reactions:

$$\begin{cases} x_{CO} = x_{CH_4} - x_{CO_2} \\ x_{H_2} = 3x_{CH_4} + x_{CO_2} \\ x_{H_2O} = -x_{CH_4} - x_{CO_2} \end{cases}$$

Consequently, the total flow rate is:

$$F_{total} = F_{total}^o + 2\,F_{CH_4}^o\left(1 + 2\,x_{CH_4}\right)$$

The kinetics reaction set is not at equilibrium. Conservation of each gas component comes from the overall continuity equation. Due to the plug flow assumption only axial variations are accounted. The energy balance equation is decomposed into two major terms. The first one corresponds to the enthalpy changes with on efficiency factor for the kinetic set, and the second one is the wall heat transfer flux. The pressure losses are based on Bernouilli equation with a main correction with a friction factor.

Fluid phase

Continuity equation

$$\begin{cases} \dfrac{d\,x_{CH_4}}{dz} = \dfrac{\Omega\,\rho_B\left(\eta_1\,r_1 + \eta_3\,r_3\right)}{F_{CH_4^0}} \\ \dfrac{d\,x_{CO_2}}{dz} = \dfrac{\Omega\,\rho_B\left(\eta_2\,r_2 + \eta_3\,r_3\right)}{F_{CH_4^0}} \end{cases}$$

Energy equation

$$\rho_g C_p u_s \frac{dT}{dz} = \rho_B \sum_1^3 \eta_i\, r_i\left(-\Delta H_i\right) - 4\frac{h_r}{d_{ti}}\left(T - T_r\right)$$

Momentum equation

$$\frac{d\,p_t}{dz} = -f\,\frac{\rho_B\,u_s^2}{d_p}$$

Inlet conditions

$$x_{CH_4}^0,\, x_{CO_2}^0,\, T^0,\, p_t^0$$

- The viscosity of water is obtained from the Chapman-Enskog theory [29].
- The overall heat transfer coefficient *hr* is obtained from the Froment and Bischoff book (pp 404-405 [27]). It takes into account the effective thermal conductivity of the bed with no flow, see Kuni and Smith [30].
- The friction factor f is calculated from the Ergun's equation [31].
- The average speed u_s is calculated from the total flow-rate:

$$u_s = \frac{RT}{p_t}\frac{F_{total}}{\Omega}$$

where Ω is the reactor cross-sectional area

Since the partial pressure gradients are limited to a very thin layer near the surface, planar geometry is studied. The reaction rates in the equations for solid phase are evaluated at the local partial pressures within the catalyst slab. Given the partial pressures of CH_4 and CO_2, all of the other concentrations can be found from the stoichiometry. The boundary conditions link the fluid phase and the solid phase.

Solid phase

Mass balance

$$\begin{cases} D_{e,CH_4}\dfrac{d^2 p_{CH_4}}{dr^2} = \rho_s\,R\,T\left(r_1 + r_3\right) \\ D_{e,CO_2}\dfrac{d^2 p_{CO_2}}{dr^2} = -\rho_s\,R\,T\left(r_2 + r_3\right) \end{cases}$$

Boundary condition

$$\begin{cases} r = 0 \Rightarrow & \dfrac{d\,p_{CH_4}}{dr} = \dfrac{d\,p_{CO_2}}{dr} = 0 \\ r = R_p \Rightarrow & p_{CH_4} = p_{CH_4,B} \quad p_{CO_2} = p_{CO_2,B} \end{cases}$$

Since effective diffusion coefficients (D_{e,CH_4} , D_{e,CO_2}) are not constant (given in appendix B), the classical analytical solution is not correct, see Levent et al [34]. Consequently, second derivative terms are evaluated by a classical centred scheme. New iterate is obtain by an application of the classical Taylor polynom formula. Many numerical tests were done and 161 nodes to discretise mass balance are required to obtain a numerical stable solution (i.e. independent of the number of nodes).

2.3 STEAM REFORMER MODEL VALIDATION

By definition of the methane conversion variable, a unitary value means that the conversion is achieved for a length of the catalyst bed of 30 cm. The main parameters used in the simulation of the steam reformer are given in Table 3. As previously detailed, the conversion variables are plotted on figure 9.

Reformer data	
Length of reformer tube	0.3 m
Inside diameter of reformer tube	0.10 m
Outside diameter of reformer tube	0.13 m

Catalyst data	
Catalyst Pellet dimension	17 x 8 x 10 mm
Pellet porosity	0.5
Pellet equivalent diameter	7.5 mm
Pellet tortuosity	3.54
Solid catalyst density	2355 kg/m^3
Catalyst bed density	1170 kg/m^3

Table 3: Steam Reformer data

At the reformer exhaust, the mole fraction of hydrogen is near to 15% and carbon monoxyde 4%. Figure 10 correspond to the 2D representation (length of catalyst bed and Pellet coordinate) of mole fraction of fuel (hydrogen and carbon monoxide) and inert gases (carbon dioxide and steam). This representation clearly shows that the dimensions of the catalyst Pellet are correct since an established state is obtained.

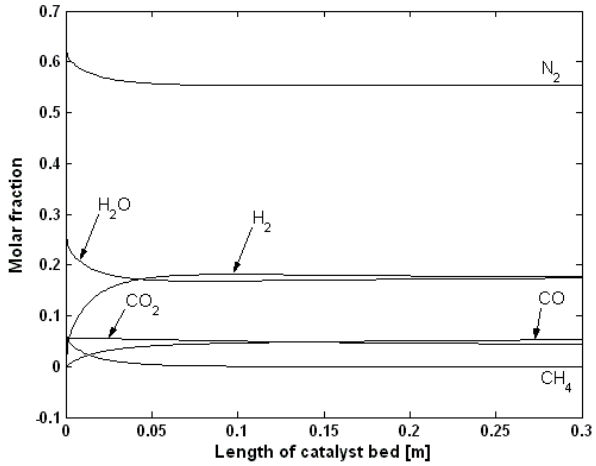

Figure 9. Evolution of molar fraction along catalyst bed

Allenby et al. [35] have achieved this system for natural gas fuelled engine with a length of catalyst bed of approximately 10 cm) and the reformer inlet temperature of 1000K. They tested three reactors and gave the measured outlet volumetric composition from the reformer. The presented model gives a good tendencies for each specie, see Figure 11.

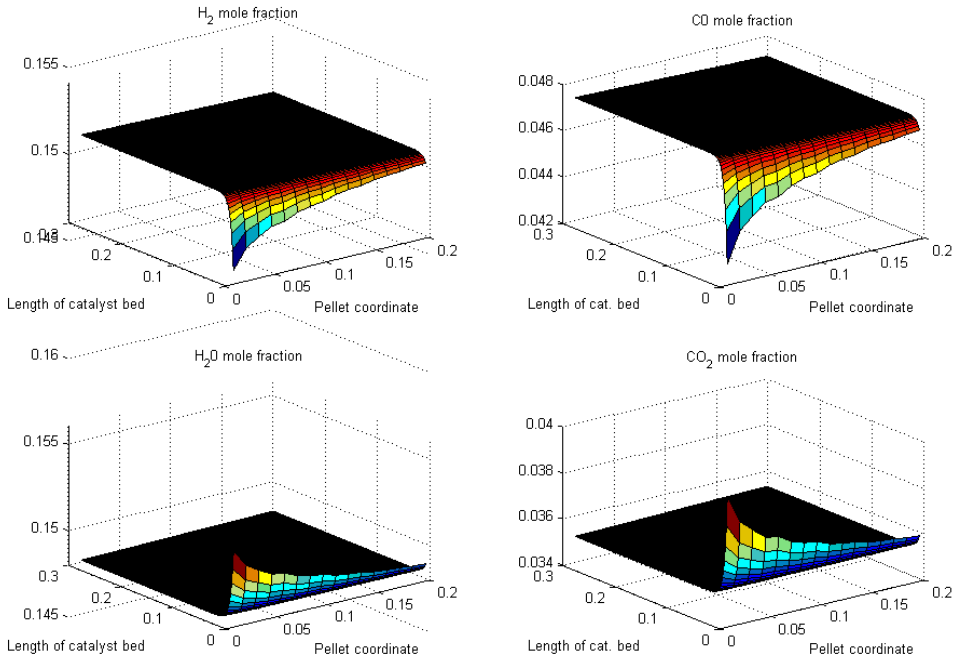

Figure 10. 2D-plot mole fraction versus length of catalyst bed *z* and radial grid *r* (pellet coordinate)

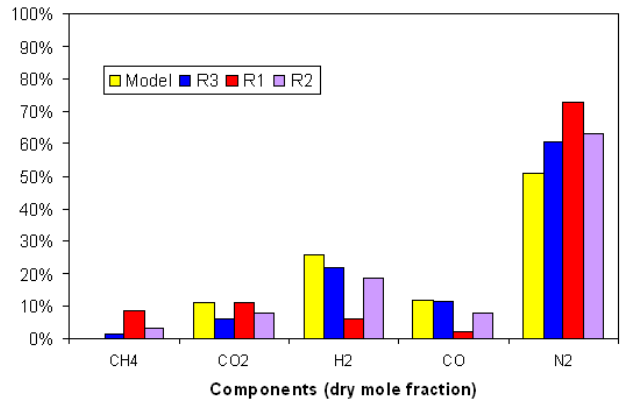

Figure 11. Comparison between Model and the Allenby's Measurement for the dry mole fraction of the reformer exhaust

3. RGR PREDICTION ON S.I. PERFORMANCES

The reformer gas recirculation is evaluated by successive numerical simulations. *SI* engine initial simulation is calculated on a fuel taken as natural gas. Those exhaust emissions are the inlet conditions for the fluid phase of steam reformer. The steam reformer exhaust is blended to natural gas for a new simulation of *SI* engine performance. This loop is stopped for two consecutive steam reformer exhaust compositions have a difference lesser than 0.5%. This stop criteria is commonly reached in 3 loops. The considered engine conditions are, weaker lean *FAR* (avoiding combustion defaults), Best Efficiency Spark Advance, 100% *WOT*.

Having of model for *SI* engine and reformer, it is possible to predict the interest of the steam reforming compared to other solution to decrease nitrous oxide in exhaust gas.

To add exhaust gas recirculation (i.e. a major blend of CO_2, H_2O and N_2) has an effect of dilution and then the in-cylinder temperature is globally lesser than without. As the mechanism of nitrous oxide depends on the formation temperature, less Nox are produced with an adding flowrate. Nevertheless, the reformer recirculation is of other nature since this gas is partially a fuel. Considering 20% of *RGR* volume flowrate as a limit, *NOx* decreasing is about 30% compared to the same *EGR* flowrate, see Figure 12. In-cylinder peak pressure is a common indicator to get an idea of *SI* performances. *EGR* and *RGR* concepts provide a significant NO_x reduction with quasi-constant *SI* performances. Greater the *RGR*, greater the interest in comparison with classical *EGR*, see Figure 13.

CONCLUSIONS

Utilisation of reformed gas recirculation as a complement to natural gas is an opportunity to optimise the *CHP* engines in term of emissions.

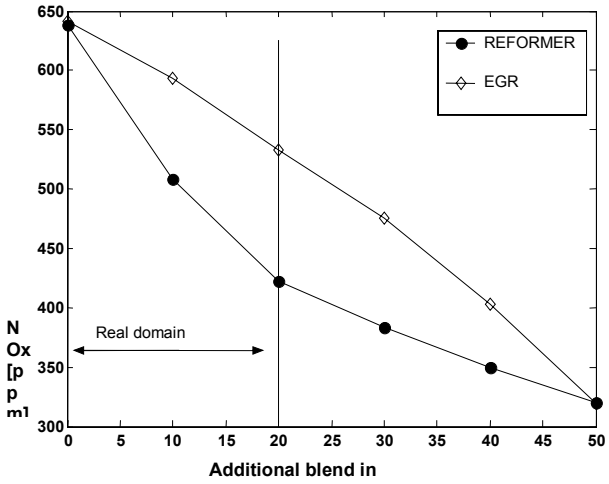

Figure 12. Nitrous oxide versus additional blends (in percentage)

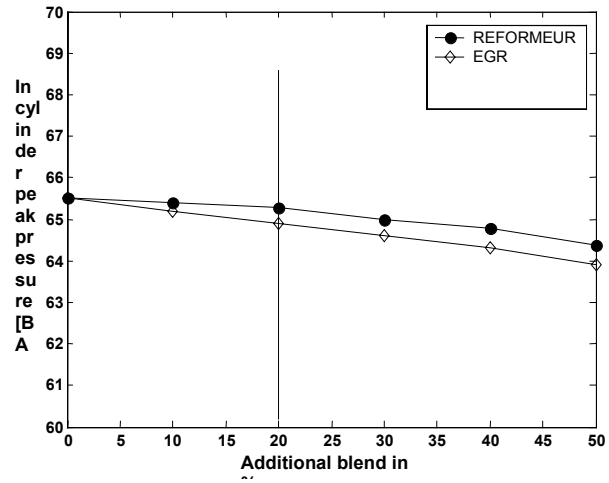

Figure 13. In-cylinder peak pressure versus additional blends (in percentage)

This conclusion is obtained by simulation of two distinct models (one for *SI* engine fuelled by natural gas and this other for steam reforming). *SI* engine model was validated in term of in-cylinder peak pressure and nitrous oxide: good match is obtained, less than 0.5%. Steam reforming model was validated on bibliography data.

Two ways to reduce nitrous oxide have been studied: exhaust and reformed gas recirculation. On *SI* engine performances and emissions, the best way seems to be *RGR*.

Important interests of *RGR* have not been underlined by this numerical approach and correspond obviously of its model limits. Firstly, under lean (or very lean) conditions, *SI* combustion is lesser and lesser stable and sometimes the combustion does not propagate. This running is called has

"motoring cycle". Tsolakis and Megaritis [5] reported that the high flame speed of hydrogen stabilise the propagation and consequently improve the performance. Secondly, using *RGR* the in-cylinder cycle to cycle dispersions are decreased (see Apostolescu and Chiriac [36]), this phenomena has its source from hydrogen use. Thirdly, to burn hydrogen must be implicated a decreasing of carbon dioxide emissions. One potential major negative aspect was not mentioned : the "knock combustion". But, lean conditions are not favourable one.

Although it is difficult to test in real conditions the *RGR* on a *CHP* plant for insurance aspect in a laboratory, more numerical studies could demonstrated the real interest of this concept.

REFERENCES

[1] Sogaard C., J. Schramm and T.K. Jensen, 2000, *Reduction of UHC-emissions from Natural Gas Fired SI-engine – Production and Application of Steam Reformed Natural Gas*, SAE Paper 2000-01-2823.

[2] Tsolakis A. and A. Megaritis, 2004, *Exhaust gas assisted of rapeseed methyl ester for reduced exhaust emissions of CI engines*, Biomass and Bioenergy 27:493-505.

[3] Hoekstra R.L., K. Collier, N. Mulligan and L. Chew, 1995, *Experimental study of a clean burning vehicle fuel*, Int. J. Hydrogen Energy, Vol 20, N°9:737-745.

[4] Zheng M., G.T. Reader and J.G. Hawley, 2004, *Diesel engine exhaust gas recirculation–a review on advanced and novel concepts*, Energy Conversion and Manag. 45 :883–900.

[5] Tsolakis A. and A. Megaritis, 2004, *Catalytic exhaust gas fuel reforming for diesel engines – effects of water addition on hydrogen production and fuel conversion efficiency*, International Journal of Hydrogen Energy 29 pp1409-1419.

[6] Jamal Y., T. Wagner and M.L. Wyszynski, 1996, *Exhaust gas reforming of gasoline at moderate temperatures*, Int. J. Hydrogen Energy, Vol 21, N°6:507-519.

[7] Fergusson C.R., 1986, *Internal Combustion Engines Applied Thermosciences*, Ed. John Wyley & Sons.

[8] Heywood J.B., 1988, *Internal Combustion Engine Fundamentals*, Mc Graw Hill.

[9] Ramos J.I., 1989, *Internal Combustion Engine Modeling*, Hemisphere Publishing Corporation.

[10] Gatowski J.A., E.N. Balles, K.M. Chun, F.E. Nelson, J.A. Ekchian and J.B. Heywood, 1984, *Heat Release Analysis of Engine Pressure Data*, SAE Paper 841359.

[11] Hohenberg G.F., 1979, *Advanced Approaches for Heat Transfer Calculations*, SAE Paper 790825.

[12] Rousseau S., 1999, *Contribution to the study of the thermodynamic cycle in lean burn natural gas engines used in cogeneration*, Ph.D. Thesis, Université de Nantes, (in french).

[13] Loper L.A. and S.R. Bell, 1994, *Simulation of a Spark Ignited Engine*, Transactions of the ASME, Journal of Internal Combustion Engines, 94-ICE-17.

[14] Eriksson L., 1999, *Spark Advance for Optimal Efficiency*, SAE Paper 1999-01-0548.

[15] Hajireza F., F. Mauss and B. Sunden, 1998, *Two Zone Model of Gas Thermodynamic State in SI Engine with relevance for knock*, The fourth International Symposium COMODIA, pp 203:208.

[16] Ishii K., T. Sasaki, Y. Urata, K. Yoshida and T. Ohno, 1997, *Investigation of Cyclic Variation of IMEP under Lean Burn Operation in Spark-Ignition Engine*, SAE Paper 972830.

[17] Miyamoto N., T. Chikahisa, T. Murayama and R. Saywer, 1985, *Description and Analysis of Diesel Engine Rate of Combustion and Performance using Wiebe's Functions*, SAE Paper 850107.

[18] Liu Z. and G.A. Karim, 1998, *Simulation of Combustion Process in Gas Fuelled Diesel Engines*, AIAA/ASME Joint Thermophysics and Heat Transfer Conference, 1:297-304.

[19] Abd Alla G.H., H.A. Soliman, A. Badr and M.F. Abd Rabbo, 2001, *Using of quasi-two Zone Combustion Model to Predict the Performance of a Dual Fuel Engine*, SAE Paper 2000-01-2936.

[20] Micklow G.J., B. Owens and M. Russels, 1994, *Cycle Analysis for fuel-induced Internal Combustion Engine Configurations*, Proceedings of ImechE, Vol 215 of *D*, pp 115-125.

[21] Bade S.O., Shrestha and G.A. Karim, 1998, *A predictive Model for Gas Fuelled Spark Ignition Engine Applications*, SAE Paper 980162.

[22] Chmela F., M. Engelmayer, R. Beran, A. Ludu, 2003, *Prediction of Heat Release Rate and NOx Emission for Large Open Chamber Engines with Spark Ignition*, 3rd Dessau Gas Engine Conference, May 22-23.

[23] Shahad Al-Janabi H. A.-K. and M. A.-R. Sadi Al-Baghadi, 1999, *A prediction study of the effect of hydrogen blending on the performance and pollutants emission of a four stroke spark ignition engine*, International Journal of Hydrogen Energy 24, 363-375.

[24] Leide B., 1994, *Residual reactivity of burnt gases in the expansion turbine of future gas turb*ines, PhD Ecole des Mines de Paris, in french.

[25] Xu J. and G.F. Froment, 1989, Methane steam reforming, methanation and water-gas shift: intrinsic kinetics, A.I.Ch.E. Journal, 33, pp88-96.

[26] Nielsen M.P. and S.K.Kaer, 2003*, Modeling a PEM Fuel Cell Natural Gas Reformer*, Conference ECOS'2003, July.

[27] Froment G.F. and K.B. Bischoff, 1990*, Chemical Reactor Analysis and Design*, ISBN 0-471-51044-0, John Wiley & Sons, second edition.

[28] de Groote A.M. and G.F. Froment, 1996, *Simulation of the catalytic oxidation of methane to synthesis gas*, Applied Catalysis A: General, 138:245-264.

[29] Chapman S. and T.G. Cowling, 1970*, The mathematical theory of non-uniform gases*, John Wilet & Sons Inc., Third edition.

[30] Kunii, D.and J.M. Smith, 1960, *Heat transfer characterisation of porous rocks*, Journal of American Institute of Chemical Engineers 6, 71–78.

[31] Ergun, S., 1952, *Fluid flow through packed columns*, Chemical Engineering Progress 48, 89–94.

[32] Cussler E.L., 1997, *Diffusion*, Cambridge University Press, Cambridge.

[33] Zalc J.M., S.C. Reyes and E. Iglesias, 2004, *The effects of diffusion mechanism and void structure on transport rates and tortuosity factors in complex porous structures*, Chemical Engineering Science 59 2947 – 2960.

[34] Levent M., G. Budak and A. Karabulut, 1998, *Estimation of concentration and temperature profiles for methane-steam reforming reaction in a porous catalyst*, Fuel Processing Technology, 55:251-263.

[35] Allenby S., W.C. Chang, A. Megaritis and M.L. Wyszynski, 2001, *Hydrogen enrichment: a way to maintain combustion stability in a natural gas fuelled engine with exhaust gas recirculation, the potential of fuel reforming*, Proc Instn Mech Engrs Vol 215 Part D N°3 pp 405-418.

[36] Apostolescu N. and R. Chiriac, 1996*, A Study of Combustion of Hydrogen-Enriched Gasoline in a Spark Ignition Engine*, SAE paper 960603.

[37] Caton, J.A., 2000, *Comparisons of instructional and complete versions of thermodynamical engine cycle simulations for spark ignition engines*, International Journal of Mechanical Engineering Education, Vol 29, N°4, pp 283-306.

[38] Douaud A., 1981, *Analyse et Optimisation à charge partielle des moteurs à quatre temps*, Pétrole et Technique (281), Juin-Juillet.

[39] Olikara C. and G.L. Borman, 1975, *A Computer Program for Calculating properties of Equilibrium Combustion Products with some Applications to I.C. engines*, SAE Paper 750468.

[42*29] *CHEMKIN collection*, 1999, Kee RJ, Rupley FM, Miller JA, Coltrin ME, Grear JF, Meekc E, Moffat HK, Lutz AE, Dixon-Lewis G, Smooke MD, Warnats J, Evans GH, Larson RS, Mitchell RE, Petzold LR, Reynolds WC, Caracotsios M, Stewardt WE, Glarborg P, Reaction Design Inc, San Diego, CA.

APPENDIX A : Two-zones thermodynamic model

The set of equations is summarised through the following 8 points, see Caton [37].

1/ Volume evolution

$$V(\theta) = V_c + \frac{\pi B^2}{4}\left(l + a(1-\cos\theta) - \sqrt{l^2 - a^2 \sin^2\theta}\right)$$

2/ Inlet-Outlet Phase

$$\frac{dm}{d\theta} = \delta_{valve}\, \frac{Cd\, A_{valve} P_{upst}}{\omega} \sqrt{\left(\frac{2\gamma}{(\gamma-1)RT_{upst}}\right)\left|Rp^{2/\gamma} - Rp^{\gamma+1/\gamma}\right|}$$

3/ State equation

Unburnt gas : $p V_u = m_u\, r_u\, T_u$

Burnt gas : $p V_b = m_b\, r_b\, T_b$

4/ First law of thermodynamic

Unburnt gas :

$$m_u\, Cv_u \frac{d\,T_u}{d\theta} = -p\,\frac{d\,V_u}{d\theta} - \frac{d\,Q_{p,u}}{d\theta} - u_u \frac{d\,m_u}{d\theta} - h_u \frac{d\,m_c}{d\theta}$$

Burnt gas :

$$m_b\, Cv_b \frac{d\,T_b}{d\theta} = -p\,\frac{d\,V_b}{d\theta} - \frac{d\,Q_{p,b}}{d\theta} - u_b \frac{d\,m_b}{d\theta} + h_u \frac{d\,m_c}{d\theta}$$

5/ Mass burning rate :

Mass fraction of burnt gas, from Chmela et al [22] :

$$\frac{d\,x_b}{d\,\theta} = \frac{\kappa}{1+\lambda\, AFR}\, \rho_b\, S_L \left(\frac{\theta}{\omega}\right)^2 (1-x_b)$$

Laminar Speed from Rousseau [12] and Shahad Al-Janabi and Sadi Al-Baghadi [23]

$$S_L = 9656 \frac{p}{p_0}^{-0.623}\, e^{\frac{-2145}{T_u}} + 0.83 \left(\frac{[H_2] + \frac{[H_2]}{([H_2]/[air])_{st}}}{[G] + \left([Air] - \frac{[H_2]}{([H_2]/[air])_{st}}\right)}\right)$$

6/ Lean burn combustion [12,38,39]

$$\phi\, FAR\, C_\alpha H_\beta O_\gamma N_\delta + (0.79\, N_2 + 0.21\, O_2) \rightarrow \sum \nu_j\, Y_j$$

$$Y_j \in \{CO_2, H_2O, N_2, O_2, CO, H_2, H, O, OH, NO, N\}$$

Coupled with Extended Zeldovitch Mechanism and Prompt Nox Model

7/ Physical properties [40] : Chemkin

8/ Wall heat exchange *:* Hohenberg et al [11]

APPENDIX B : Effective Diffusion Coefficient

The molecular diffusion coefficient of the species must be calculated, which depends on temperature and have both a molecular and a Knudsen diffusion component. In one hand, Knudsen diffusion coefficients are from the standard kinetic theory.

$$D^K = \frac{d_p}{3}\sqrt{\frac{8\,R\,T}{\pi\, M}}$$

where d_p is the pore diameter. In other hand, molecular diffusion coefficients are from Cussler's book [32] and are binary diffusion coefficients for CO_2 in H_2O and CH_4 in H_2O.

$$D^m_{CH_4} = 0.292\left(\frac{T}{307.7}\right)^{1.5} \text{ and } D^m_{CO_2} = 0.202\left(\frac{T}{307.5}\right)^{1.5}$$

Composite diffusion coefficients D^B for each size range are obtained from geometric mean (called "Bosanquet formula", see Zalc et al [33] of the ordinary and Knudsen diffusion coefficients.

$$D^B_{CH_4} = \left(\frac{1}{D^K_{CH_4}} - \frac{1}{D^m_{CH_4}}\right)^{-1} \quad \text{for methane, respectively}$$

$$D^B_{CO_2} = \left(\frac{1}{D^K_{CO_2}} - \frac{1}{D^m_{CO_2}}\right)^{-1} \quad \text{for carbon dioxide.}$$

By introducing the porosity, or internal void fraction ε, and the tortuosity τ, one gets the effective diffusion coefficient for each species, D_{e,CH_4} and D_{e,CO_2}.

$$D_{e,CH_4} = D^B_{CH_4}\,\frac{\varepsilon}{\tau} \text{ and } D_{e,CO_2} = D^B_{CO_2}\,\frac{\varepsilon}{\tau}$$